Selenium-vacancy-mediated NiCoSe nanoplatforms with NIR-II amplified nanozyme for Methicillin-resistant *Staphylococcus aureus*-infected pneumonia

Liqin Wu,[1,2] Lida Jin,[3] Xintong Zou,[3] Xiaojun He,[4,*] Yuanrong Dai,[2,*] and Jianan Huang[1,*]

[a] Department of Respiratory Medicine, the First Affiliated Hospital of Soochow University, Suzhou, Jiangsu, 215006, China

[b] Department of Pulmonary Medicine, The Second Affiliated Hospital and Yuying Children's Hospital of Wenzhou Medical University, Wenzhou, Zhejiang, 325000, China

[c] Department of Anesthesiology. The First Affiliated Hospital of Wenzhou Medical University, Wenzhou, Zhejiang, 325035, China

[d] National Engineering Research Center of Ophthalmology and Optometry, Eye Hospital, Wenzhou Medical University, Wenzhou 325027, China

All authors have approved the final version of this manuscript.

*Address correspondence: hexiaojun@wmu.edu.cn (X. He), dairy@126.com (Y. Dai), and huang_jian_an@163.com (J. Huang).

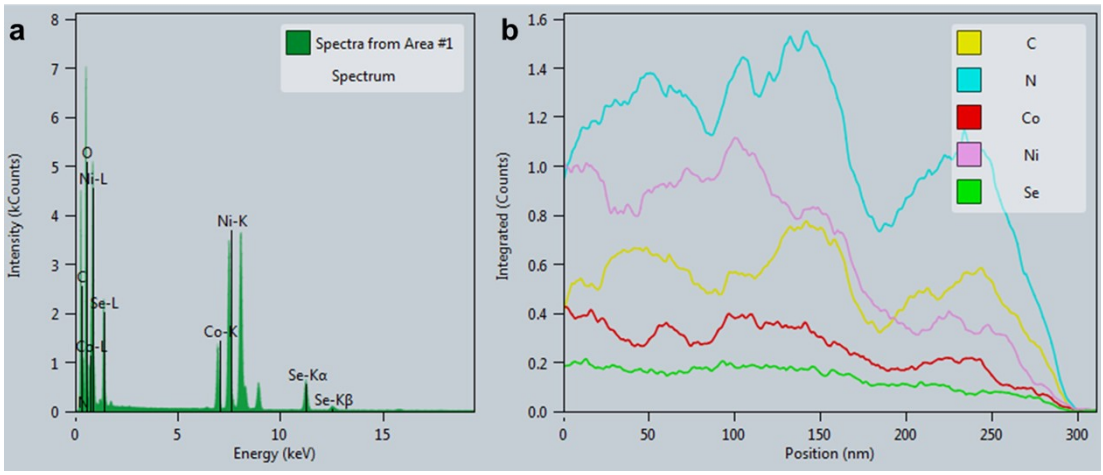

Fig. S1. (a) X-ray energy dispersive spectrum of NiCoSe. (b) The location of the EDS line scan is shown in the dotted yellow arrow in Figure 1d.

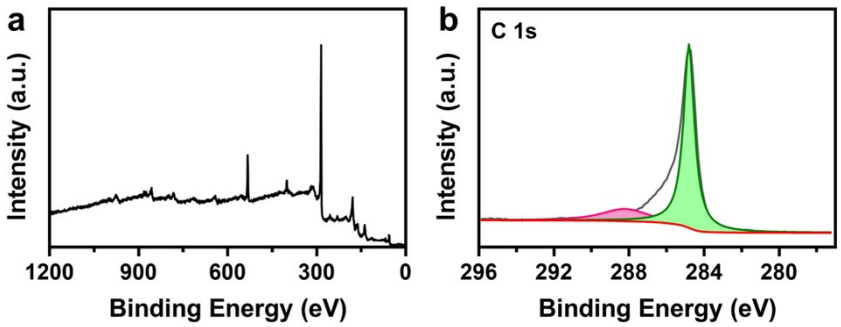

Fig. S2. (a) XPS survey spectra of NiCoSe. (b) High-resolution XPS spectra of C 1s regions.

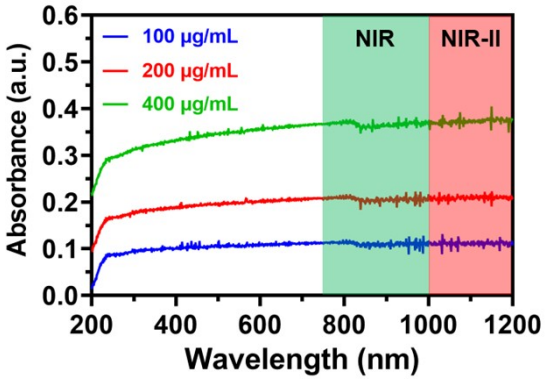

Fig. S3. UV-vis-NIR absorption spectra of NiCoSe dispersions at different concentrations. The inserted images represent the first near-infrared biowindow (750-1000 nm) and the second near-infrared biowindow (1000-1200 nm).

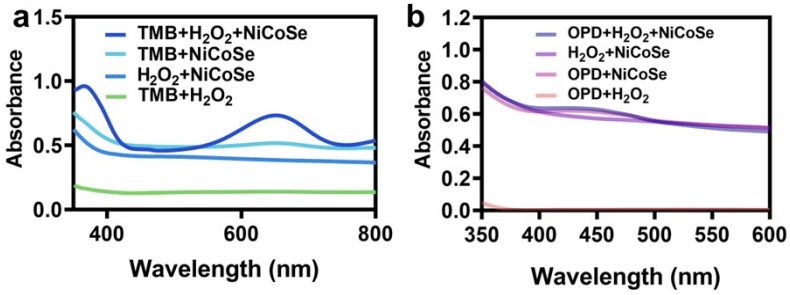

Fig. S4. The enzyme-like activity of NiCoSe under different conditions using TMB (a) and OPD (b) as substrate.

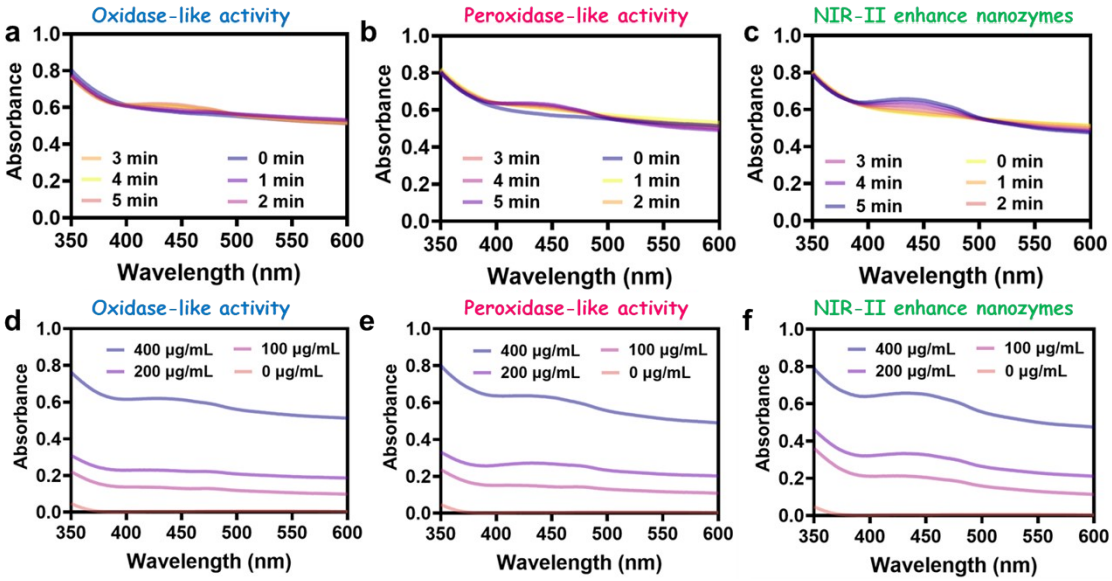

Fig. S5. Dual enzyme-like activities of NiCoSe. OXD-like (a) and POD-like (b) activities of NiCoSe with time-dependent using OPD as substrate. (c) NIR-II enhanced the POD-like activity of NiCoSe at different times. OXD-like (d) and POD-like (e) activities of NiCoSe with concentration-dependent using OPD as substrate. (f) NIR-II enhanced the POD-like activity of NiCoSe with different concentrations.

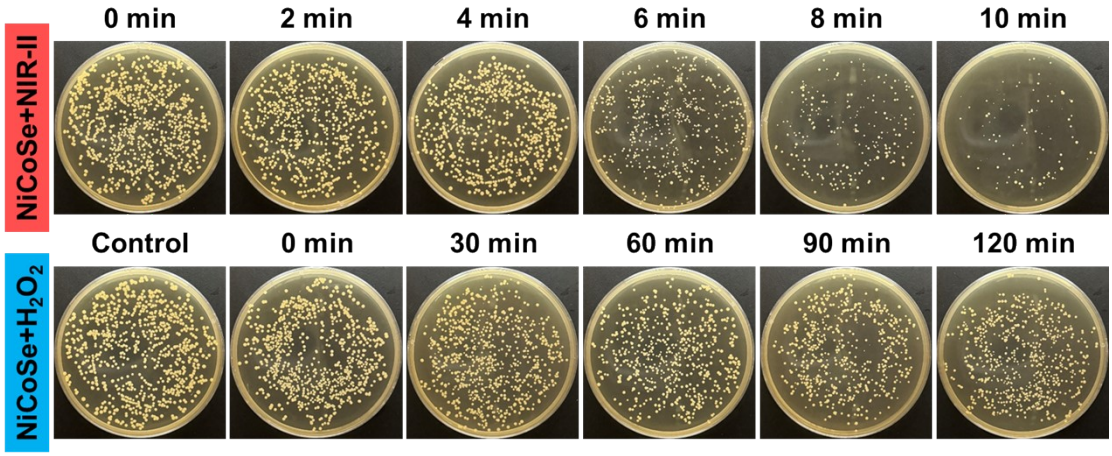

Fig. S6. MRSA inhibition effects after treatment with NIR-II (1064 nm, 1.0 W/cm^{-2}) and H_2O_2 (0.1 mM) under different times.

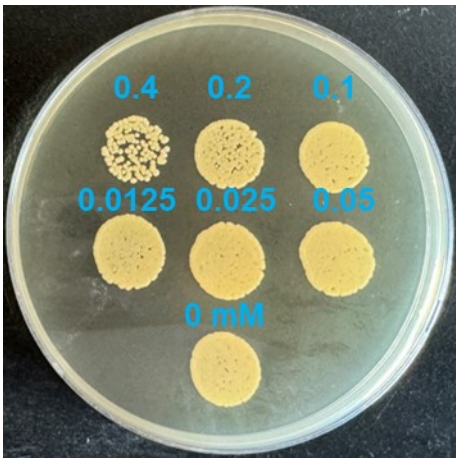

Fig. S7. MRSA inhibition effects after treatment with different concentrations of H_2O_2 from 0 to 1.0 mM.

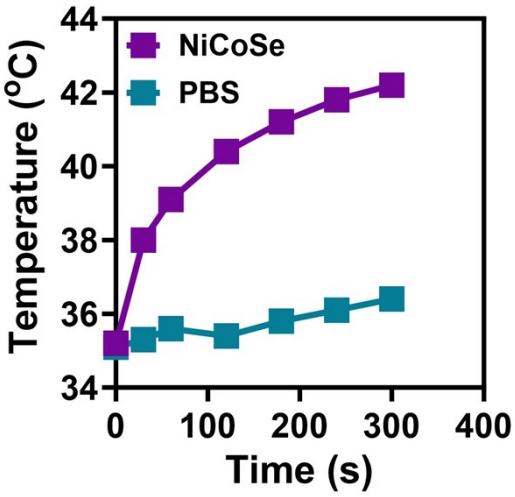

Fig. S8. Local body temperature of mice in different periods under irradiation of NIR-II (1064 nm, 1.0 W/cm^{-2}) with and without NiCoSe (400 μg/mL).

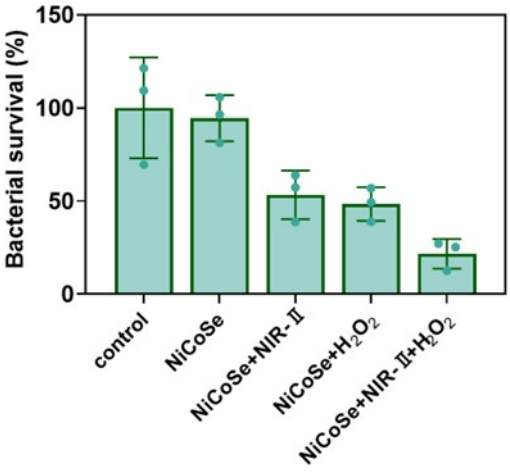

Fig. S9. The corresponding statistical analysis of relative bacterial viability in lung tissue with different treatments.

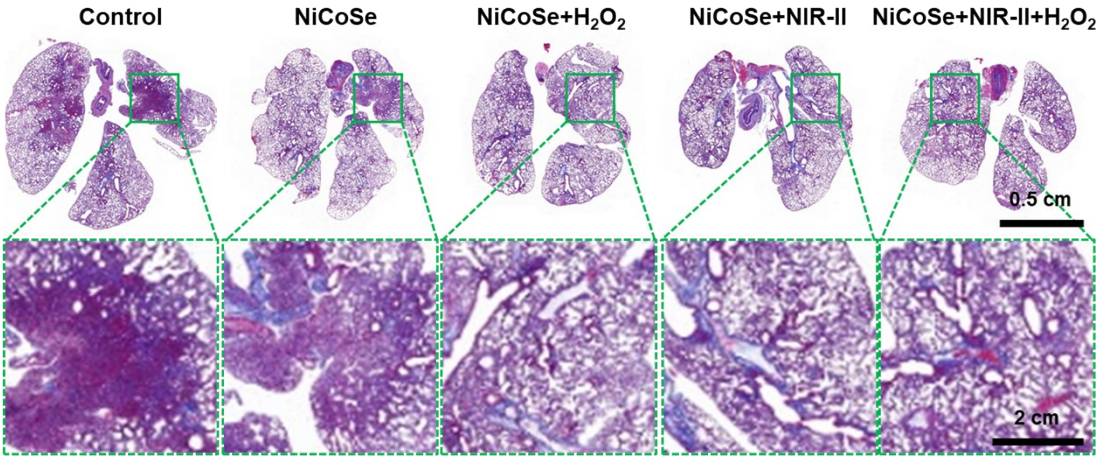

Fig. S10. Masson staining of lung tissues collected from the abscess areas in different treatments.

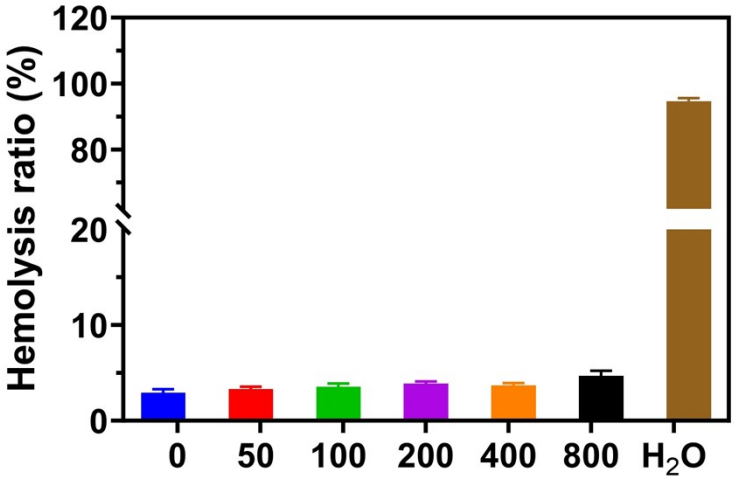

Fig. S11. Representative photographs and quantitative analysis of hemolysis activity of NiCoSe dispersions with different concentrations (0 μg/mL to 800 μg/mL).

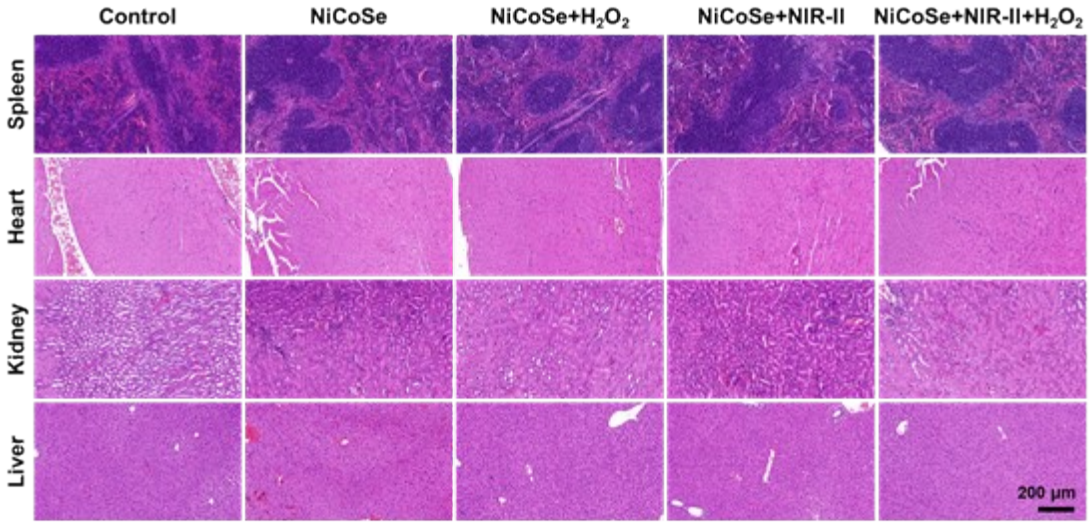

Fig. S12. H&E staining images of the main organs (heart, liver, spleen, and kidney) of mice after receiving various therapies.